Goal-directed action preparation in humans entails a mixture of corticospinal neural computations

Corey G. Wadsley[1,2], Thuan Nguyen[3], Chris Horton[1], Ian Greenhouse[1,2,*]

[1]Action Control Lab, Department of Human Physiology, University of Oregon, Eugene, Oregon, USA
[2]Institute of Neuroscience, University of Oregon, Eugene, Oregon, USA
[3]School of Public Health, Portland State University-Oregon Health and Science University, Portland, Oregon, USA

**Corresponding author*: Ian Greenhouse (img@uoregon.edu)
Department of Human Physiology
181 Esslinger Hall,
1525 University St.
Eugene, OR 97403

Running title: Human action preparation entails corticospinal neural computations

Keywords: Human, Motor cortex, Action preparation, Gain modulation, Noninvasive brain stimulation

Key points:

- Neural computations determine what information is transmitted through brain circuits.
- We investigated whether the motor system uses computations similar to those observed in sensory systems by noninvasively stimulating the corticospinal pathway in humans during goal-directed action preparation.
- We discovered physiological evidence that corticospinal projections to behaviorally relevant muscles exhibit nonlinear gain computations, while projections to behaviorally irrelevant muscles exhibit linear suppression.
- Our findings suggest that certain computational principles generalize to the human motor system and serve to enhance the contrast between relevant and background neural activity.
- These results indicate that neural computations during goal-directed action preparation may support motor control by increasing signal-to-noise within the corticospinal pathway.

Abstract: The seemingly effortless ability of humans to transition from thinking about actions to initiating them relies on sculpting corticospinal output from primary motor cortex. This study tested whether canonical additive and multiplicative neural computations, well-described in sensory systems, generalize to the corticospinal pathway during human action preparation. We used non-invasive brain stimulation to measure corticospinal input-output across varying action preparation contexts during instructed-delay finger response tasks. Goal-directed action preparation was marked by increased multiplicative gain of

corticospinal projections to task-relevant muscles and additive suppression of corticospinal projections to non-selected and task-irrelevant muscles. Individuals who modulated corticospinal gain to a greater extent were faster to initiate prepared responses. Our findings provide physiological evidence of combined additive suppression and gain modulation in the human motor system. We propose these computations support action preparation by enhancing the contrast between selected motor representations and surrounding background activity to facilitate response selection and execution.

Introduction

Humans are experts at using their fingers for goal-directed actions to interact with their environment effectively (Xu *et al.*, 2024). This behavioral repertoire is supported by a specially evolved neural architecture comprising excitatory and inhibitory mechanisms that sculpt corticospinal (CS) pathway output during goal-directed action preparation (Prut & Fetz, 1999; Duque *et al.*, 2017; Bundt & Huster, 2024). The anatomy of the distributed cortical and spinal circuits that modulate CS output during action preparation and execution is well characterized (Wang *et al.*, 2017; Derosiere & Duque, 2020). However, the precise neural computations that unfold throughout the transition from action preparation to execution are not (Churchland & Shenoy, 2024). Candidate computations have been proposed but are based on neuronal circuit modeling and experimental evidence from investigations of non-motor neural systems and behaviors (Greenhouse, 2022). Thus, it is unclear whether computational principles from non-motor circuits generalize to the human motor system and account for the top-down modulation of CS output during action preparation.

Influential models of goal-directed action preparation postulate that inhibition of the CS pathway acts as a functional gate, with the removal of inhibition allowing selective excitatory signals to pass through to the musculature and produce intended actions (Zagha *et al.*, 2015; Soteropoulos, 2018). Yet, physiological recordings from non-human primates have provided mixed evidence for gating mechanisms within the CS pathway (Merchant *et al.*, 2008; Kaufman *et al.*, 2010, 2013). Indeed, (dis)inhibition supports a variety of computations other than gating in non-motor neural circuits (Katzner *et al.*, 2011; Lee *et al.*, 2012; Mischler *et al.*, 2023). Multifaceted computations are also likely required in the motor system since movements are not static but instead defined by various kinetic and kinematic features that characterize a given action. Therefore, alternative interpretations to the functional gating account should

be considered to better explain how preparatory activity determines CS pathway excitability to shape ensuing actions.

The selection and timing of goal-directed actions may be determined by neural computations similar to, or bound to, those of non-motor circuits (Beste *et al.*, 2023). Such computations, responsible for sculpting descending signals, are expected to manifest in distinct patterns of CS input-output during goal-directed action preparation. One candidate computation is gain modulation, defined in studies of sensory processing as a multiplicative (non-linear) change in a system‘s input-output relationship and a proposed feature of canonical normalization processes within the brain (Hillyard *et al.*, 1998; Salinas & Thier, 2000; Pi *et al.*, 2013). Computational models indicate gain modulation is important in determining primary motor cortex (M1) output (Pouget & Snyder, 2000; Stroud *et al.*, 2018), the predominant source of descending signals of the human CS tract (Welniarz *et al.*, 2017). Additive modulation, defined by a linear shift across an input-output spectrum (Silver, 2010), is an alternative candidate computation that may account for CS input-output adjustments during action preparation. Computational models of additive modulation indicate effective changes in an input-output threshold (Mitchell & Silver, 2003), whereby widespread suppression can stabilize a neuronal population by reducing the preponderance of spontaneous firing (Ferguson & Cardin, 2020). During action preparation, additive modulation may function as the ‘quiet before the storm’ to prepare the CS pathway for impending descending commands.

A third alternative is that multiplicative and additive computations are concurrent and complementary. A precedent for synergistic computations can be found in the vision system. Extending a divisive normalization framework (Carandini & Heeger, 2012) to the motor system, the activity of a motor representation selected for action can be divided by the summed activity of alternative non-selected and bystander motor representations, producing enhanced signal-to-noise (Georgopoulos & Stefanis, 2007; Greenhouse, 2022). A combination of multiplicative and additive computations could serve to separate figure from ground in a manner resembling neural sensory processing and would be consistent with a general neurocomputational principle throughout the human nervous system akin to exponentiation, linear filtering, and divisive normalization (Carandini & Heeger, 2012).

In this study, we tested the presence of multiplicative and additive computations in human CS input-output during the behavioral state change from rest to action preparation of goal-directed finger movements (Figure 1a). We hypothesized that goal-directed action preparation involves a concurrent gain increase and additive suppression to enhance the contrast between selected and background motor representations along the CS pathway.

Methods

Participants

Forty-five young, neurologically healthy adults volunteered to participate. The study was approved by the institutional review board of the University of Oregon and performed with each participant's understanding and written consent. All participants self-reported as right-handed and were screened for contraindications to TMS before data collection. Five participants were excluded from data collection due to a high resting motor threshold (≥ 60% maximum stimulator output), making the TMS input-output protocol unfeasible. An additional participant was excluded after data collection due to noncompliance with task instructions. The remaining 39 participants completed the entire study and were available for all statistical analyses (20 females, 19 males; mean age 20.3 yrs., range 18 to 30 yrs.).

Task protocol

Goal-directed action preparation was assessed with an instructed-delay two-choice reaction time task (Figure 1b). Participants were seated comfortably in front of a computer monitor (59 Hz refresh rate, ~60 cm viewing distance) with their hands palm-down and shoulder-width apart on a table surface. The task was designed using Psychtoolbox-3 integrated with MATLAB (R2019b; The MathWorks) and a custom response board (Makey Makey v.1.2; Joylabz) for accurate timing. Stimuli were synchronized with task equipment through an analog-to-digital data-acquisition module (PCI-6620; National Instruments) and verified during later offline analyses using photodiode recordings. The default task display consisted of a blank grey background at trial onset. A fixation cue (centered white rectangle, 20 x 20 pixels) appeared 0.3 s after trial onset. A warning cue appeared 1 to 1.5 s after trial onset (randomly drawn from a uniform distribution) and indicated the forthcoming response (hollow leftward or rightward pointed

triangle, 140 x 150 pixels). An imperative stimulus (triangle filling white) appeared 0.9 s after the warning cue and lasted until a button press was recorded or 0.8 s elapsed. Each trial was followed by an intertrial interval (blank grey background) after the imperative stimulus and lasted until 7.6 s had elapsed from the trial onset.

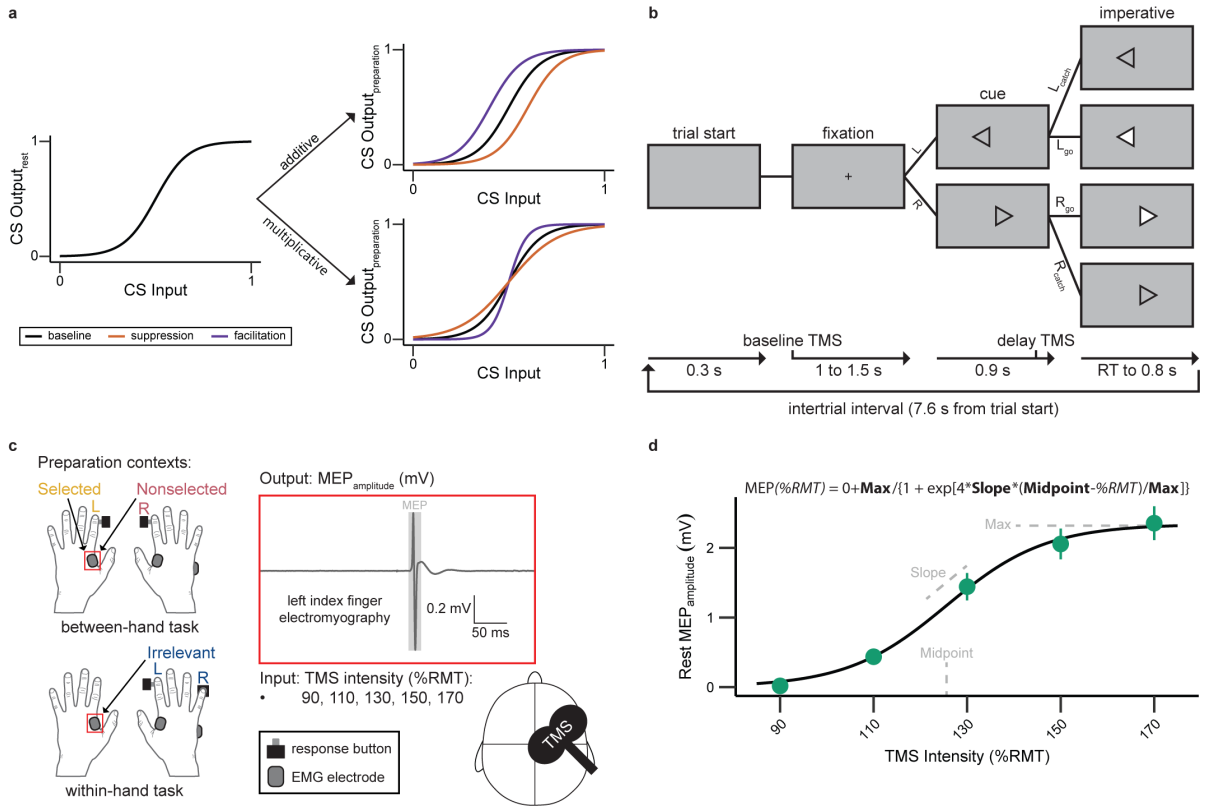

Figure 1: Assessment of human CS input-output during goal-directed action preparation. **a**, Corticospinal (CS) input-output can exhibit additive and/or multiplicative modulation from baseline rest to a preparatory state. **b**, Goal-directed action preparation was assessed with an instructed-delay two-choice reaction time task requiring left (L) or right (R) responses. Most trials were go trials during which the imperative stimulus appeared until a reaction time (RT) was recorded or 0.8 s elapsed. A subset of catch trials (~8%) was included to prevent participants from predicting imperative stimulus onset. **c**, The experiment was split into between-hand and within-hand tasks, enabling the assessment of CS output from the left index finger with single-pulse transcranial magnetic stimulation (TMS) when the targeted motor representation was at baseline and when it was selected, nonselected, or irrelevant for action preparation. Here, input was TMS intensity relative to a participant's resting motor threshold (%RMT), and output was the amplitude of ensuing motor evoked potentials (MEPs). **d**, CS input-output curves derived from pre-task resting state MEP data and fit with a population-based nonlinear mixed effects model using a three-parameter Boltzmann function. Green dots and error bars indicate mean MEP amplitude ± SEM at each TMS intensity. Dashed grey lines illustrate parameter estimates.

The experiment was split into between-hand and within-hand choice tasks (Figure 1c). Both tasks were performed in the same session with a counterbalanced order across participants. Participants were provided a short break in between tasks. Left and right imperative stimuli required button presses from the left and right index fingers during the between-hand choice task and button presses from the right index and pinky fingers during the within-hand task. Participants were instructed to relax during the

108 fixation period, to prepare but not execute the forthcoming response during the cue period, and to
109 execute the cued response as fast as possible when the imperative stimulus was presented. A subset of
110 no-go catch trials (i.e., no imperative stimulus; 8% of trials) was included to discourage participants from
111 responding prematurely in anticipation of the imperative stimulus. For each task, there was a total of 238
112 trials evenly distributed across left and right imperative stimuli and split across 4 blocks alternating
113 between 59 and 60 trials. The entire experiment lasted 2.5 hours on average.

114 *Electromyography*

115 Electrophysiological muscle activity was assessed with surface electromyography (EMG)
116 recorded using bipolar Ag-AgCl surface electrodes (Delsys Incorporated). EMG was collected from the
117 left and right FDI and the right *abductor digiti minimi* (ADM) hand muscles, which corresponded to the
118 primary agonist muscles for between-hand$_{left}$ (left FDI), between-hand$_{right}$ and within-hand$_{left}$ (right FDI),
119 and within-hand$_{right}$ (right ADM) choice alternatives. An additional EMG electrode was positioned over the
120 C3 vertebra of the neck to record TMS artifacts, and a shared ground electrode was positioned on the left
121 ulnar styloid process. EMG activity was amplified (×1000), bandpass filtered (20 – 450 Hz), and sampled
122 at 5000 Hz with a Bagnoli-8 amplifier (Delsys Incorporated) connected to a BNC-2090A terminal block
123 (National Instruments). EMG data were recorded on each trial for 4 s from onset using the MATLAB-
124 based VETA toolbox (Jackson & Greenhouse, 2019) and stored for later offline analyses.

125 *Transcranial Magnetic Stimulation*

126 Physiological changes in CS input-output during goal-directed action preparation were assessed
127 with single-pulse TMS delivered using a 70 mm figure-of-eight coil connected to a MagStim 200^2
128 stimulator (MagStim Ltd.). The coil was oriented to induce a posterior-to-anterior flowing current in the
129 underlying cortical tissue. The optimal coil position ('motor hotspot') over right M1 for eliciting a motor
130 evoked potential (MEP) in the left FDI was then assessed and marked on the scalp. The resting motor
131 threshold (RMT) of left FDI was defined as the minimum stimulator output required to elicit an MEP
132 amplitude of at least 0.05 mV at rest using a maximum-likelihood parameter estimation by sequential
133 testing strategy (Silbert *et al.*, 2013). TMS was delivered across a range of stimulation intensities relative

134 to a participant's RMT (90%, 110%, 130%, 150%, and 170%; 14 stimuli per intensity) to derive CS input-
135 output curves, with MEP peak-to-peak amplitude used as an index of CS output (Bestmann & Duque,
136 2016). The TMS input-output protocol was performed at baseline (start of fixation period) and during
137 action preparation (100 ms before the imperative stimulus) in the between-hand and within-hand tasks.
138 The task design enabled assessment of CS output to the left FDI muscle during baseline and during
139 action preparation when the muscle was selected (i.e., the agonist for prepared action), nonselected, or
140 task-irrelevant (Figure 1c). Nonselected refers to the context in which the left index finger was a choice
141 alternative in the task but was not cued to respond on a given trial, while task-irrelevant refers to the
142 context in which the left index finger was never a choice alternative in the task.

143 *Dependent measures*

144 Data were preprocessed using the VETA toolbox in two stages. In the first stage, EMG bursts,
145 MEPs, and TMS artifacts were marked with the automated detection *findEMG.m* function. In the second
146 stage, data was manually reviewed using the *visualizeEMG.m* function to ensure the accuracy of EMG
147 measures. Here, EMG data contaminated by artifacts were rejected, and EMG burst onset timings were
148 adjusted when required. Dependent measures were then extracted with custom scripts in MATLAB.
149 Behavioral measures were analyzed from non-TMS trials to avoid the influence of TMS on response
150 times. Go success was calculated as the percentage of go trials where a correct response was made
151 within 0.8 s from imperative stimulus onset. Catch trial success was calculated as the percentage of no-
152 go trials where the cued response was withheld correctly. Trials with button press RTs less than 100 ms
153 or EMG RTs less than 50 ms were then marked as premature responses and excluded from subsequent
154 analyses (M = 2.2 % of all trials). There was a strong positive correlation between button press and EMG
155 RT (r = 0.68, P < 0.001), as such, we report only EMG-based RTs for subsequent analyses since it is free
156 from electromechanical delays.

157 Dependent measures from stimulated trials during the between-hand and within-hand choice
158 tasks included pre-trigger root mean square EMG and MEP amplitudes. Trials with TMS were excluded
159 when pre-trigger root mean square EMG activity exceeded 30 μV in a -30 to -5 ms pre-TMS window or

when outlier MEP amplitudes were identified, defined as values more than three times the scaled median absolute deviation from the median (*M* = 11.4 % of stimulated trials). The mean pre-TMS root mean square EMG activity of the left FDI was calculated from the remaining trials for each preparation context, collapsed across stimulation intensities. CS output of the left FDI was calculated as the mean MEP peak-to-peak amplitude for each preparation context and stimulation intensity separately.

Statistical analyses

Statistical analyses were performed using R software (Version 4.3.0). The normality of data and model-averaged residual plots were visually inspected where appropriate. Logarithmic transformations were used in the case of non-normally distributed data. The alpha level was set to 0.05 for statistical significance. P-values for pairwise post-hoc comparisons were adjusted for multiple comparisons using the Benjamini-Hochberg method to control the false discovery rate at 5%. In-text data are presented as nontransformed mean ± standard deviation unless otherwise specified.

Go and catch trial success rates were analyzed using an omnibus Friedman test with the factor of Response (within-hand$_{left}$, within-hand$_{right}$, between-hand$_{left}$, between-hand$_{right}$) to verify task performance was high and consistent across response alternatives. EMG RT was analyzed using a linear mixed-effects model with fixed effects of Task (within-hand, between-hand) and Side (left, right) and random effect of participant specificity to verify participants were responding fast and to determine any differences between tasks and response alternatives.

We employ a population-based nonlinear mixed-effects model to determine the influence of action preparation context on the CS input-output relationship. A modified three-parameter Boltzmann sigmoid function (Heusser *et al.*, 2021) was used to model the nonlinear sigmoidal input-output relationship between TMS intensity and MEP amplitude (Kukke *et al.*, 2014):

$$MEP(\%RMT) = 0 + Max/\{1 + exp[4 * Slope * (Midpoint - \%RMT)/Max]\}$$

where MEP(%RMT) is the predicted MEP peak-to-peak amplitude at a given TMS intensity, calculated as a function of Max (upper plateau), Midpoint (inflection point), and Slope (maximum rate of change) input-

185 output parameter estimates. Here, the Midpoint and Slope parameters indicate additive and multiplicative
186 computations, respectively (Figure 1d). The lower plateau of CS input-output was constrained to 0 mV for
187 greater biological plausibility (i.e., MEP amplitude cannot be negative and should always be 0 mV at a 0%
188 TMS intensity) and provided a better fit of the data compared to an unconstrained model (constrained
189 AIC: 1307.5, unconstrained AIC: 1317.0).

190 Initial parameter estimates for the nonlinear mixed-effects models were derived from pre-task
191 resting state data to ensure independence between model optimization and statistical analyses.
192 Specifically, initial estimates were set to mean MEP amplitude at 170% RMT for Max, median stimulation
193 intensity for Midpoint (i.e., 130% RMT), and the linear gradient between 110% and 130% RMT for Slope
194 based on visual inspection of averaged MEP amplitude data. We then applied nonlinear least squares
195 modeling (*nls* function in R) with these initial parameter estimates to obtain corresponding optimal
196 parameter estimates of 2.34 mV for Max, 125.6 %RMT for Midpoint, and 0.055 mV/%RMT for Slope with
197 an iterative numerical integration procedure. These estimates were subsequently applied to a model of in-
198 task TMS data (*nlme* function in R). Max, Midpoint, and Slope parameters were estimated from this
199 random intercept model to account for participant variability. The model was then updated with the fixed
200 effect of Context (baseline, irrelevant, nonselected, selected) to examine the influence of action
201 preparation context on CS input-output. Updated models with the fixed effect of Task Order (within-hand
202 first, between-hand first) or Sex (male, female) were also included to determine any effects of task order
203 or participant sex on CS input-output parameters.

204 A linear mixed-effects model with a fixed effect of Context (baseline, irrelevant, nonselected,
205 selected) was used to confirm modulation of CS input-output was not attributable to shifts in pre-TMS root
206 mean square EMG activity.

207 We estimated a Gain Index *post priori* for each participant to capture interindividual differences in
208 CS input-output Slopes and evaluate whether observed context-dependent gain adjustments correlated
209 with task behavior. Direct parameter estimations could not be used from the population-based model
210 since variance is shared across participants and, thus, interindividual differences between contexts

211 derived from the population-based model are not meaningful. As such, we estimated the Gain Index by 1)
212 extracting the estimated Midpoint for each context and participant separately, 2) determining the two
213 neighboring input TMS intensities (e.g., 110% and 130% RMT if the estimated Midpoint was within these
214 bounds), 3) estimating the linear gradient (slope) between the mean MEP amplitudes from their individual
215 data corresponding to the selected input TMS intensities, and 4) calculating the estimated difference
216 between task-relevant contexts (average of selected and nonselected contexts) and task-irrelevant
217 contexts, normalized to baseline, i.e. $(slope_{relevant} - slope_{irrelevant})/slope_{baseline}$. Thus, a greater Gain Index
218 reflects a larger difference in the Slope of CS input-output between task-relevant and task-irrelevant
219 preparation contexts. The association between mean EMG RT, collapsed across all response types
220 (average non-stimulated trial number per response type: between-$hand_{left}$ 10.2 ± 2.0; between-$hand_{right}$
221 10.7 ± 1.8; within-$hand_{left}$ 10.4 ± 2.3; within-$hand_{right}$ 10.9 ± 2.0), and the Gain Index was then tested using
222 Pearson's correlation.

223 **Results**

224 CS input-output parameters changed during goal-directed action preparation in a context-
225 dependent manner (Figure 2a). The Context model provided a better fit of the data than the Null model
226 (Context AIC: 1264.3, Null AIC: 1312.9). Importantly, there was no effect of Context on pre-TMS muscle
227 activity ($F_{3,144}$ = 0.58, P = 0.629), which was below 10 μV in all contexts (baseline 5.5 ± 2.5 μV; irrelevant
228 5.8 ± 4.0 μV; nonselected 5.5 ± 2.7 μV; selected 5.8 ± 2.5 μV). Thus, participants' muscles rested during
229 action preparation, and differences in alpha motoneuron depolarization did not explain the modulation of
230 CS input-output (Devanne *et al.*, 1997).

231 *CS gain increases during response preparation for task-relevant representations*

232 The Slope of CS input-output differed significantly across Context ($F_{3,730}$ = 4.26, P = 0.005).
233 Estimated Slope was greater in the selected context compared to baseline ($F_{1,730}$ = 5.42, P = 0.040) and
234 the irrelevant context ($F_{1,730}$ = 9.76, P = 0.011). Estimated Slope in the nonselected context was also
235 greater than the irrelevant context ($F_{1,730}$ = 5.87, P = 0.040) but not baseline ($F_{1,730}$ = 2.79, P = 0.143).
236 There were no significant differences between baseline and irrelevant ($F_{1,730}$ = 0.95, P = 0.397) as well as

between nonselected and selected contexts ($F_{1,730}$ = 0.23, P = 0.628). Thus, context-dependent multiplicative modulation of CS input-output was explained by an increase of Slope when the stimulated motor representation was selected or nonselected for forthcoming action (i.e., task-relevant) compared to baseline or when it was task-irrelevant (Figure 2b). Such nonlinear increases in sensitivity to excitatory inputs are associated with response potentiation across sensory systems (Wood *et al.*, 2017). Multiplicative gain modulation may be important for maximizing signal-to-noise and, computationally, can extend the dynamic range of neuronal operations (Mitchell & Silver, 2003; Shine *et al.*, 2018). Of note is that increased Slope was observed in both the selected and nonselected preparation contexts, indicating a general role of gain modulation in potentiating task-relevant motor representations rather than promoting effector-specific action selection. Overall, gain modulation may be pertinent for establishing the pool of candidate actions.

The Max of CS input-output also differed significantly across Context ($F_{3,730}$ = 24.04, P < 0.001). Estimated Max was greater in the selected context compared to irrelevant ($F_{1,730}$ = 14.62, P = 0.001) and nonselected ($F_{1,730}$ = 6.44, P = 0.034) contexts, which did not differ from each other ($F_{1,730}$ = 1.89, P = 0.204). There were no differences between baseline and other contexts (all P > 0.050). Thus, CS output maximum was greater during selected than nonselected and irrelevant contexts, but not baseline (Figure 2c). This pattern differed from that observed for the Slope and indicates the dynamic range of excitability in the CS pathway is influenced by more than gain adjustments alone.

Additive suppression of CS input-output in nonselected and task-irrelevant preparatory contexts

The Midpoint of CS input-output differed significantly across Context ($F_{3,730}$ = 11.48, P < 0.001). Estimated Midpoint was greater in the irrelevant context than baseline ($F_{1,730}$ = 7.00, P = 0.012) and the selected context ($F_{1,730}$ = 18.54, P < 0.001). Estimated Midpoint in the nonselected context was also greater than baseline ($F_{1,730}$ = 9.65, P = 0.004) and the selected context ($F_{1,730}$ = 25.32, P < 0.001). There was no significant difference between nonselected and irrelevant ($F_{1,730}$ = 0.05, P = 0.828) and between baseline and selected contexts ($F_{1,730}$ = 2.50, P = 0.137). Thus, context-dependent modulation of CS input-output was explained by an additive rightward shift of the Midpoint when the stimulated motor

representation was task-irrelevant or nonselected for the forthcoming action compared to when it was selected (Figure 2d). The additive increase of the Midpoint during nonselected and irrelevant contexts was also greater than baseline, consistent with inhibition of CS input-output relative to intertrial rest (Derosiere & Duque, 2020). This nonspecific and apparently uniform suppression of irrelevant and nonselected motor representations may reflect widespread noise reduction within the CS pathway (Greenhouse *et al.*, 2015). These findings extend previous studies of preparatory inhibition and are consistent with a mechanism for enhancing the contrast of selected motor representations through the suppression of background activity.

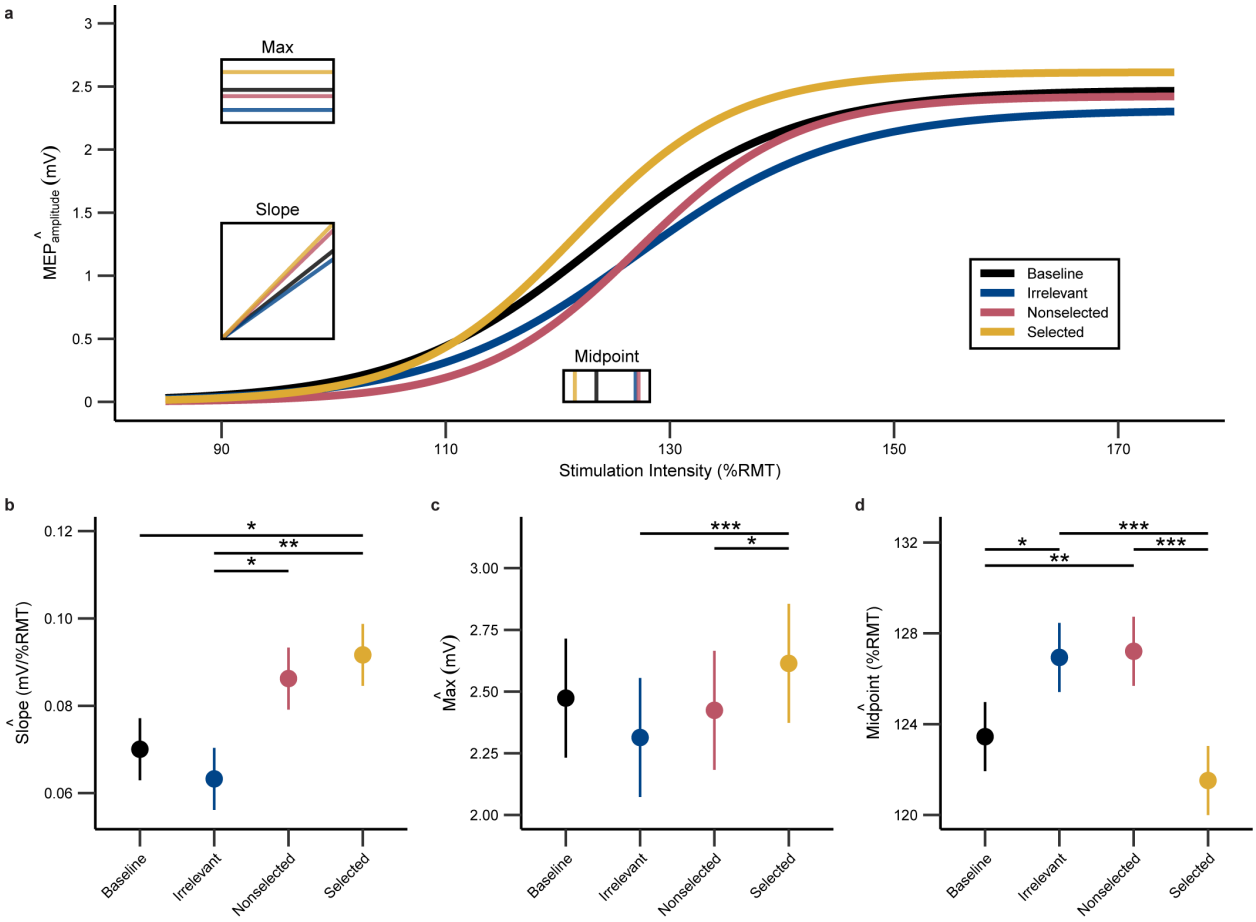

Figure 2: Modulation of CS input-output across goal-directed action preparation contexts. **a**, CS input-output curves across action preparation contexts. Insets indicate the estimated Max, Slope, and Midpoint parameters. **b**, Estimated Slope was greater in the selected context compared to baseline and irrelevant, greater in the nonselected context than irrelevant, with no significant differences between baseline and irrelevant or between nonselected and selected contexts. **c**, Estimated Max was greater in the selected context compared to the irrelevant and nonselected contexts, which did not differ from each other, with no differences between baseline and any other contexts. **d**, Estimated Midpoint was greater in the irrelevant and nonselected contexts compared to baseline and the selected context, with no significant differences between nonselected and irrelevant or between baseline and selected contexts. Data ranges represent mean ± SEM of the model-derived parameters in panels b – d, where the standard error reflects the precision of the estimated coefficients.

Preparatory suppression during goal-directed action preparation

Preparatory suppression, expressed as a reduced MEP amplitude relative to baseline, was observed during the irrelevant context across all stimulation intensities (110: $W = 615$, $P = 0.004$; 130: $W = 573$, $P = 0.029$; 150: $W = 608$, $P = 0.005$; 170: $W = 616$, $P = 0.004$), only at the 110 %RMT stimulation intensity during the nonselected context (110: $W = 644$, $P = 0.001$; 130: $W = 501$, $P = 0.372$; 150: $W = 411$, $P = 1.000$; 170: $W = 446$, $P = 1.000$), but at no stimulation intensity during the selected context (110: $W = 393$, $P = 1.000$; 130: $W = 238$, $P = 0.100$; 150: $W = 271$, $P = 0.296$; 170: $W = 280$, $P = 0.382$). Thus, preparatory suppression was observed across the entire input spectrum in the irrelevant context, only at the lower end of the input spectrum in the nonselected context and at no part of the input spectrum in the selected context (Figure 3a).

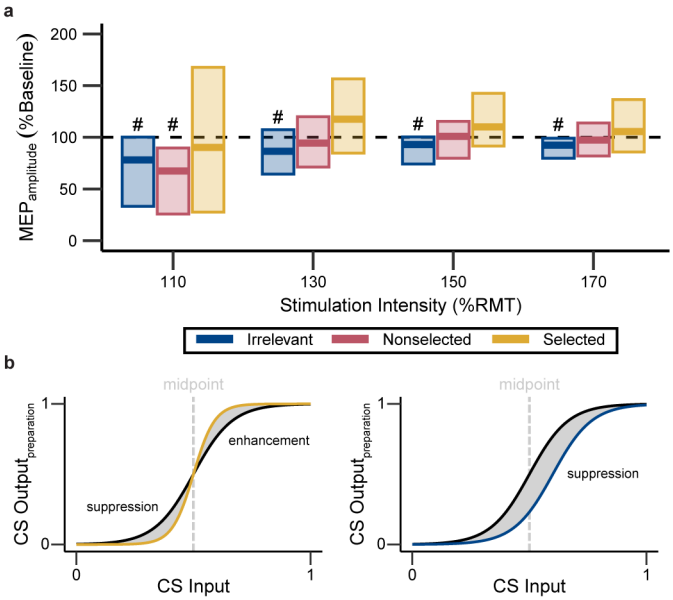

Figure 3: Preparatory suppression during goal-directed action preparation. **a**, Preparatory suppression, expressed as a reduced MEP amplitude relative to baseline, was observed during the irrelevant context across all stimulation intensities, only at the 110 %RMT stimulation intensity during the nonselected context, and at no stimulation intensity during the selected context. Crossbar boxes indicate median hilows and the dashed horizontal line indicates baseline MEP amplitude. Statistical results were obtained from paired Wilcoxon-signed rank tests of mean MEP amplitude against baseline. **b**, Conceptual overview of how CS input-output modulation can reflect preparatory suppression or enhancement depending on CS input and modulation. Here, assuming fixed alternative parameters, a multiplicative increase would be captured as preparatory suppression or enhancement at input intensities below or above the midpoint, respectively. In contrast, an additive increase (i.e., rightward shift) would be captured as preparatory suppression irrespective of the input intensity relative to the midpoint.

Gain modulation of CS input-output across preparatory contexts is associated with reaction time

Participants responded accurately and quickly during the behavioral tasks. There were no significant differences in accuracy across the response options during either go (Go: $X^2_3 = 5.08$, $P = 0.166$) or catch ($X_2^3 = 3.93$, $P = 0.269$) trials, with a high average trial success indicating that participants performed the tasks correctly (Figure 4a). Reaction time (RT), calculated based on EMG burst onset, was measured during task trials without TMS to avoid the direct influence of stimulation on motor output

(Foltys *et al.*, 2001). For EMG RT during non-stimulated trials, there was a significant fixed effect of Task ($F_{1,114}$ = 10.18, P = 0.002), with faster responses in the within-hand compared to the between-hand task. There was no fixed effect of Side ($F_{1,114}$ = 0.17, P = 0.684) or a Task × Side interaction ($F_{1,114}$ = 2.88, P = 0.092). Thus, responses were faster when the prepared action involved a within-hand choice between the fingers of the dominant hand compared to a between-hand choice. However, RTs remained fast across all response alternatives (Figure 4b). Importantly, RTs were correlated between the two tasks (R = 0.38, P = 0.001), indicating individuals differed reliably in their RTs. There was a significant negative Pearson correlation between the Gain Index and EMG RT from non-TMS trials (R = -0.32, P = 0.045), whereby participants with a larger gain modulation index had faster RTs (Figure 4c). That is, participants who exhibited greater gain adjustments in the form of slope differences between task-relevant and task-irrelevant behavioral contexts were faster to initiate responses.

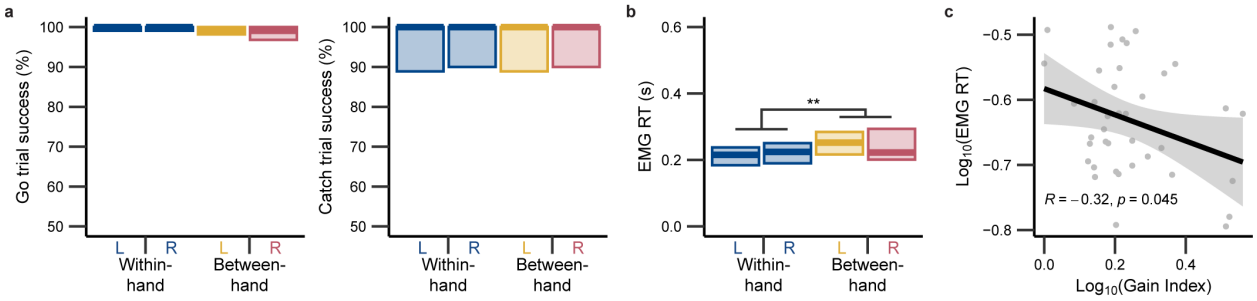

Figure 4: Behavioral performance and relationship to CS input-output gain modulation. **a**, Accuracy during go (left) and catch (right) trials for which there was no significant effect of Response type on either measure. **b**, Response initiation times based on EMG were faster during the within-hand compared to the between-hand task. **c**, There was a significant negative Pearson correlation between Gain Index and EMG RT from non-TMS trials whereby participants with greater gain in task-relevant than task-irrelevant action preparation contexts were faster responders. Crossbar boxes indicate median hilows in all panels.

CS input-output is not affected by participant sex or task order

CS input-output curves derived from the Sex model did not provide a better fit of the data than the null model (Sex AIC: 1319.1, Null AIC: 1312.9). There were no significant effects of Sex on estimated Max ($F_{1,736}$ = 0.61, P = 0.434), Slope ($F_{1,736}$ = 0.27, P = 0.605), or Midpoint ($F_{1,736}$ = 2.85, P = 0.092) CS input-output parameters. CS input-output curves derived from the Order model also did not fit the data better than the null model (Order AIC: 1320.1). There were no significant effects of Order on estimated Max ($F_{1,736}$ = 0.04, P = 0.844), Slope ($F_{1,736}$ < 0.01, P = 0.944), or Midpoint ($F_{1,736}$ = 0.02, P = 0.876) CS

input-output parameters. Thus, neither participant Sex nor task order influenced CS input-output during goal-directed action preparation (Figure 5).

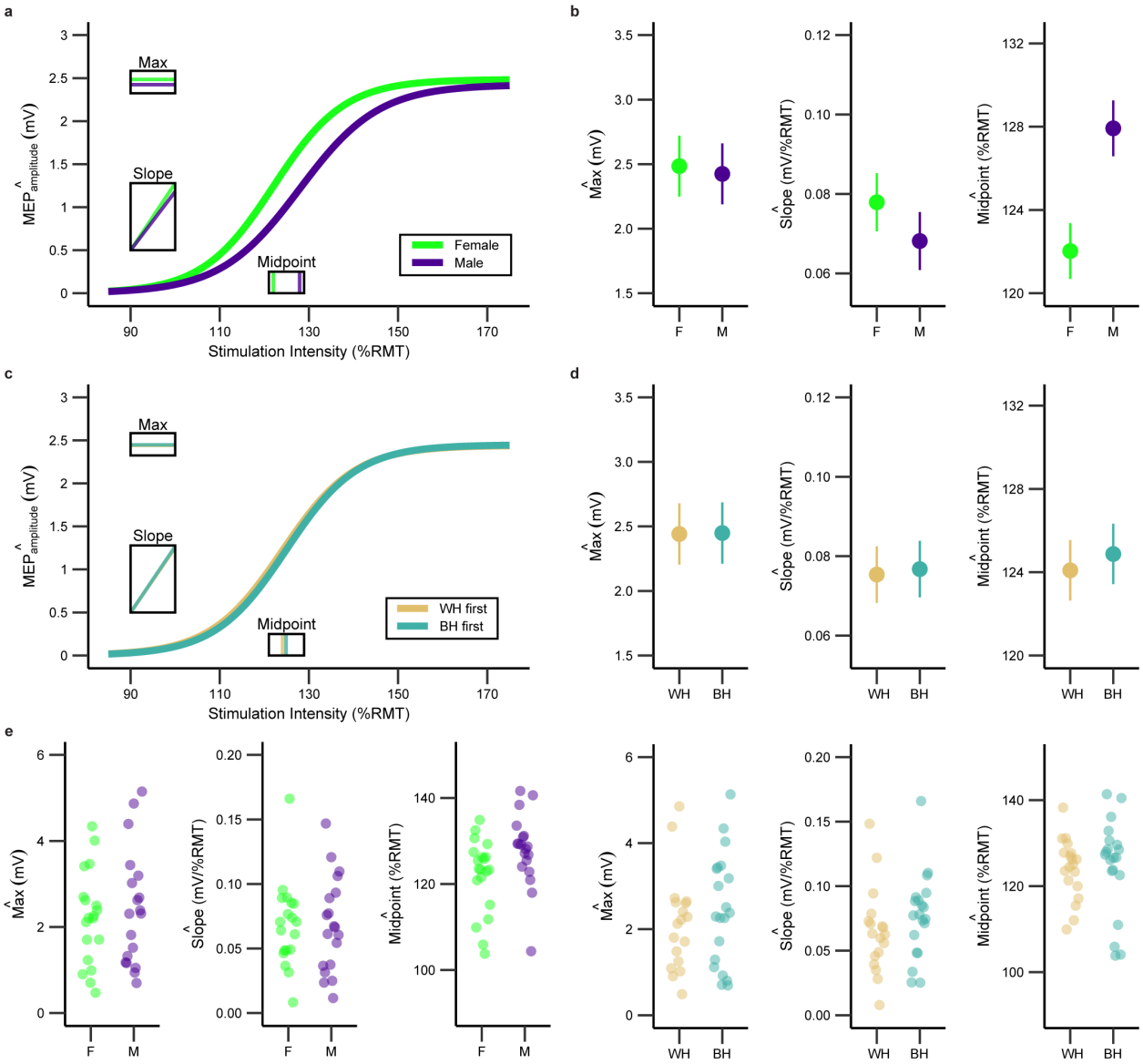

Figure 5: Modulation of CS input-output across participant sex and task order. **a**, CS input-out curves derived from the Sex model. **b**, There were no significant effects of Sex on estimated Max, Slope, or Midpoint CS input-output parameters. **c**, CS input-output curves derived from the Order model. **d**, Task order (WH: within-hand first; BH: between-hand first) had no significant effects on estimated Max, Slope, or Midpoint CS input-output parameters. **e**, Extracted participant-wise estimates of Max, Slope, and Midpoint parameters for between-subjects effects of Sex (*left*) and Order (*right*). Insets in subpanels a and c indicate estimated population means for the Max, Slope, and Midpoint parameters. Data ranges in subpanels b and d represent mean ± SEM of the model-derived parameters, where the standard error reflects the precision of the estimated coefficients.

Discussion

The present study provides novel physiological evidence of multiplicative and additive neural computations within the human CS pathway during goal-directed action preparation. Specifically, we showed that the gain of behaviorally relevant motor representations (selected and non-selected) increases against a background of additive suppression of nonselected and task-irrelevant motor representations during goal-directed action preparation. Furthermore, the magnitude of gain modulation was associated with behavioral output, such that stronger modulators were faster responders. Below, we discuss the implications of these findings for understanding state-dependent computations within the human CS pathway during motor control.

Computational parallels between sensory and motor systems during action preparation

First, the findings indicate canonical computations well-described in sensory cortices (Salinas & Sejnowski, 2001; Mitchell & Silver, 2003; Silver, 2010) generalize to the human motor system. Previous work has established feature-based attention modulates gain within visual cortices (Treue & Trujillo, 1999), and normalization in the human visual system further supports attentional processes by theoretically separating figures from the ground (Bloem & Ling, 2019). Similar gain adjustments have been observed in the auditory cortex to increase spectrotemporal contrast (Rabinowitz *et al.*, 2011). Computational models of auditory (Mischler *et al.*, 2023) and visual (Polack *et al.*, 2013) sensory systems further indicate specific roles of gain for normalization and may mirror the contrast enhancement mechanism we propose operates within the CS pathway during action preparation. Such state-dependent gain adjustments for contrast enhancement could facilitate the transmission of descending signals along the CS pathway, similar to models of basal ganglia output for action selection (Nambu *et al.*, 2002). Importantly, while sensory and motor systems differ in their representational content and anatomy, they share critical functional similarities for guiding behavior (Hatsopoulos & Suminski, 2011). Therefore, contrast enhancement via simultaneously increased gain of behaviorally relevant and suppression of background neural representations may be a canonical motif for sculpting cortical circuit output.

The current findings also align with recurrent neural network models of the non-human primate motor cortex that indicate a specific role of gain modulation in moderating movement features such as speed (Stroud *et al.*, 2018). Such models are typically based on electrophysiological recordings from a neuronal subpopulation in a target region acquired without experimental control over the input strength to the efferent motor pathway. Here, by controlling the input intensity and tailoring it to each participant, we provide corroborative physiological evidence for these models by demonstrating that gain modulation along the human CS pathway during a preparatory state facilitates the execution of subsequent actions. Based on our data, we propose that increased gain of task-relevant motor representations occurs against a backdrop of suppressed nonselected and irrelevant motor representations to enhance the contrast between selected and bystander motor representations (Greenhouse *et al.*, 2015). We theorize this extension to existing models further promotes the initiation of prepared responses by increasing signal-to-noise within the CS pathway via divisive normalization (Figure 6). Our data can also inform computational models of the motor cortex by providing useful information about the dynamic range of physiological outputs and behavioral relationships in a human model. Translation of the context-dependent approach to other model systems can help evaluate whether CS input-output adjustments during an output-null (preparatory) motor state hasten the transition to an output-potent (execution) motor state (Hannah *et al.*, 2018; Churchland & Shenoy, 2024).

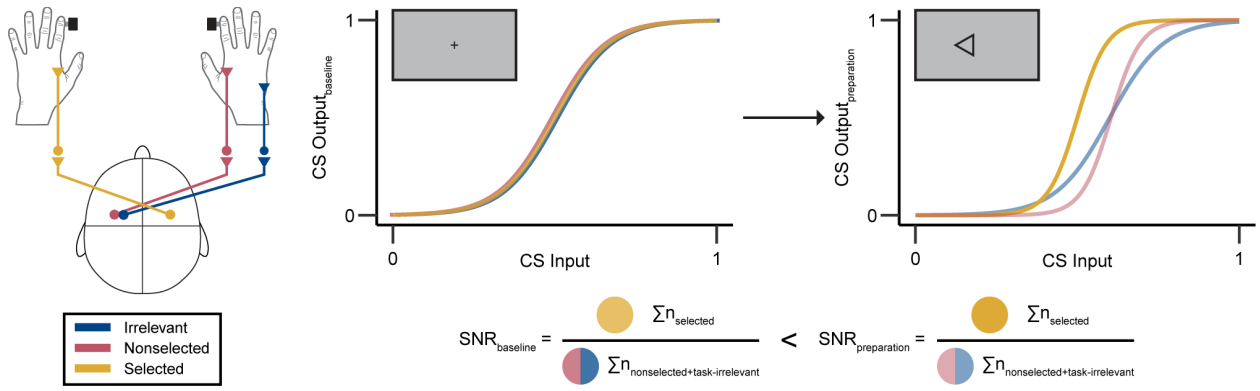

Figure 6: Theorized role of divisive normalization during goal-directed action preparation. CS input-output during action preparation depends upon task contexts. Schematized CS input-output plots represent the multiplicative increase in the selected and nonselected contexts and the additive increase in nonselected and task-irrelevant contexts. Speculatively, complementary multiplicative and additive changes can enhance the signal-to-noise ratio (SNR) between selected and bystander motor representations through divisive normalization to improve the fidelity of descending CS commands during action preparation.

Context-dependent computations with common coding frameworks

Context-dependent computations during goal-directed action preparation may fit within cognitive 'common coding' frameworks. These frameworks posit that human action control tasks are supported by internal representations ('event files') of stimulus-response relationships and their sensory effects (Hommel, 2009). Accordingly, action preparation entails retrieving an event file that triggers integrated neuronal processing across nonmotor and motor brain regions to prime action execution (Beste *et al.*, 2023). We observed neurophysiological evidence of corticospinal input-output computations recapitulated from sensory systems during action preparation, which may suggest a perception-action common code between motor and nonmotor systems. The current results, conceptualized within a common code framework, indicate that event files may have widespread motoric effects on not only the CS pathway to effectors involved directly in stimulus-response bindings but also suppression of task-irrelevant CS effector representations. In a somewhat homologous manner, modulation of sensory feedback during action control occurs at both spinal and supraspinal levels and can include a mixture of gain and suppression computations (Azim & Seki, 2019). Binding the motor command to anticipated perceptual feedback may occur via common gain modulation and suppression processes, with up-or-down regulation of neural pathways contingent upon their behavioral relevance (Frings *et al.*, 2020). Event file bindings are likely strong in the instructed-delay response task we employed; however, it is important to note that we did not set out to test event files explicitly and did not manipulate binding versus retrieval processes. Nevertheless, our findings raise the interesting possibility that gain increases in CS output during goal-directed action preparation are reciprocal to gain decreases in cutaneous feedback (Seki & Fetz, 2012) but coupled to gain increases in proprioceptive feedback during action execution (Confais *et al.*, 2017). Future work can investigate whether such changes arise from a common descending command.

Reevaluating context-dependent preparatory suppression across the CS input spectrum

An interesting observation from the current study was the lack of MEP suppression in the selected context. Previous TMS studies have observed *preparatory suppression* (i.e., reduced MEP amplitude below baseline during action preparation) across selected, nonselected, and task-irrelevant

427 contexts, albeit variably (Bundt & Huster, 2024). Our finding of enhanced CS gain in task-relevant
428 contexts may appear in conflict with inhibitory accounts (Ibáñez *et al.*, 2020). However, previous studies
429 often used a TMS intensity of ≤ 120 %RMT and, thus, only captured CS output at the lower end of the
430 input spectrum. By using a range of TMS intensities, we could model the entire CS input-output function,
431 providing a more complete picture of the underlying processes. Mathematically, both additive and
432 multiplicative changes in a sigmoidal input-output function would have complex effects on whether
433 context-dependent modulation is captured as suppression or enhancement when input intensity is below
434 or above the Midpoint (Figure 3b). We speculate that previous evidence of preparatory suppression of
435 task-relevant motor representations may result from TMS intensities below the CS input-output Midpoint.
436 Importantly, TMS may not mimic endogenous input to the CS pathway when transitioning from action
437 preparation to execution, which remains open for further investigation.

438 *Neural basis of context-dependent gain adjustments along the CS pathway*

439 Simultaneous gain adjustments and the suppression of background activity along the entire CS
440 pathway may rely on cooperative cortical, subcortical, and spinal mechanisms. For example, subcortical-
441 cortical projections from the thalamus to the prefrontal cortex selectively influence signal (figure) and
442 noise (ground) to guide cued behavior in the context of uncertainty via two distinct intracortical
443 mechanisms (Mukherjee *et al.*, 2021). Similar motifs may exist in thalamic projections to M1 to modulate
444 CS output (Halassa & Sherman, 2019). According to this framework, both increased gain of selected
445 motor representations and suppressed background activity would arise from a modulatory influence of
446 intracortical inhibitory circuits (Ferguson & Cardin, 2020). Alternatively, inhibition of background activity
447 may reflect the engagement of CS projections to spinal inhibitory neurons to suppress muscles that, if
448 activated, would interfere with the execution of the prepared action (Griffin & Strick, 2020). Computations
449 may also be mediated directly by spinal motoneurons, as MEPs measured with surface EMG exhibit
450 sigmoidal input-output properties, but individual spinal motor unit discharge rates exhibit linear input-
451 output properties (Devanne *et al.*, 1997). Summations across pools of spinal motoneurons operating
452 around the subliminal fringe may contribute to nonlinear transformations at the population level (Di
453 Lazzaro *et al.*, 1999), producing the sigmoidal shape modeled in our data. This account indicates that

454 population-level activity of spinal motoneurons operating more closely to an activation threshold during
455 action preparation could be responsible for the context-dependent gain changes we observed,
456 independent of cortical mechanisms. However, evidence of altered corticospinal input-output properties,
457 such as elevated gain in Parkinson's disease (Bologna *et al.*, 2018) and reduced maximum MEP output
458 after stroke (Buetefisch *et al.*, 2018), underscores the importance of cortico-subcortical mechanisms.
459 Therefore, it is likely that the observed CS input-output computations depend on cooperative cortical and
460 spinal mechanisms rather than a single stage in the pathway.

461 *Limitations & Future Directions*

462 The present study has some limitations. Using motor-evoked potentials (MEPs) elicited by TMS
463 provides an accurate assay of CS output. However, when probed with single-pulse TMS, MEP
464 modulation can arise from various mechanisms along the entire CS pathway, including intracortical,
465 transcortical, subcortical, and spinal mechanisms (Duque *et al.*, 2017), which may have unique roles in
466 action preparation (Derosiere & Duque, 2020). Thus, while we demonstrate that various computations
467 manifest in CS output, we cannot disentangle the level of the motor system in which they arise. Future
468 experiments will be able to determine at which level within the CS pathway these computations occur by
469 leveraging multimodal approaches, such as paired-pulse TMS, to characterize better the multifaceted
470 neuronal response to noninvasive brain stimulation and by studying clinical populations known to have
471 CS input-output irregularities. Another limitation relates to in-task TMS only being delivered at baseline or
472 a fixed time point late during action preparation. Limiting the temporal sampling was an important
473 methodological choice to collect a reliable number of trials for accurate CS input-output modeling across
474 various contexts. However, the time course of the observed computations during the transition from
475 action preparation to execution remains unclear. Future experiments may employ methods to sample CS
476 input-output effectively to enable a greater temporal resolution during action preparation (e.g., Alavi et al.,
477 2019).

Conclusion

The present study aimed to test the presence of multiplicative and additive computations in human CS input-output during goal-directed action preparation. We provided physiological evidence that goal-directed action preparation of finger responses entails a mixture of input-output computations within the human motor system. These computations are context-dependent, characterized by gain increases in task-relevant motor representations against a backdrop of suppression in bystander motor representations, potentially facilitating action initiation through contrast enhancement. The recapitulation of canonical neural computations across motor and non-motor neuronal circuits suggests that these processes may generalize throughout the human nervous system.

Additional information

Data availability statement: The data and reproducible code support this study's findings will be made publicly available in OSF upon publication, reference number osf.io/837ms.

Acknowledgments: The authors thank Kate Bakken, Mitch Fisher, Charlie Lewkowitz, Hayami Nishio, Michelle Ortman, and Tania Sarabia for their help with data collection and preprocessing. The authors also thank Luca Mazzucato and Richard Ivry for their helpful feedback on this manuscript.

Author contributions: Conceptualization, C.G.W and I.G.; Methodology, C.G.W, T.N., and I.G.; Formal Analysis, C.G.W. and T.N.; Investigation, C.G.W. and C.H.; Writing – Original Draft, C.G.W. and I.G.; Writing – Reviewing & Editing, C.G.W, T.N., C.H., and I.G.; Visualization, C.G.W.; Supervision, I.G.; Funding acquisition, I.G.

Competing interests: The authors declare no competing interests.

Funding: This research was supported by NIH grant NINDS R01NS123115.

499 **References**

500 Alavi SMM, Goetz SM & Peterchev A V. (2019). Optimal Estimation of Neural Recruitment Curves Using
501 Fisher Information: Application to Transcranial Magnetic Stimulation. *IEEE Transactions on Neural*
502 *Systems and Rehabilitation Engineering* **27,** 1320–1330.

503 Azim E & Seki K (2019). Gain control in the sensorimotor system. *Curr Opin Physiol* **8,** 177–187.

504 Beste C, Münchau A & Frings C (2023). Towards a systematization of brain oscillatory activity in actions.
505 *Commun Biol* **6,** 137.

506 Bestmann S & Duque J (2016). Transcranial Magnetic Stimulation. *The Neuroscientist* **22,** 392–405.

507 Bloem IM & Ling S (2019). Normalization governs attentional modulation within human visual cortex. *Nat*
508 *Commun* **10,** 5660.

509 Bologna M, Guerra A, Paparella G, Giordo L, Alunni Fegatelli D, Vestri AR, Rothwell JC & Berardelli A
510 (2018). Neurophysiological correlates of bradykinesia in Parkinson's disease. *Brain* **141,** 2432–
511 2444.

512 Buetefisch CM, Revill KP, Haut MW, Kowalski GM, Wischnewski M, Pifer M, Belagaje SR, Nahab F,
513 Cobia DJ, Hu X, Drake D & Hobbs G (2018). Abnormally reduced primary motor cortex output is
514 related to impaired hand function in chronic stroke. *J Neurophysiol* **120,** 1680–1694.

515 Bundt C & Huster RJ (2024). Corticospinal excitability reductions during action preparation and action
516 stopping in humans: Different sides of the same inhibitory coin? *Neuropsychologia* **195,** 108799.

517 Carandini M & Heeger DJ (2012). Normalization as a canonical neural computation. *Nat Rev Neurosci* **13,**
518 51–62.

519 Churchland MM & Shenoy K V. (2024). Preparatory activity and the expansive null-space. *Nat Rev*
520 *Neurosci* **25,** 213–236.

521 Confais J, Kim G, Tomatsu S, Takei T & Seki K (2017). Nerve-Specific Input Modulation to Spinal
522 Neurons during a Motor Task in the Monkey. *The Journal of Neuroscience* **37,** 2612–2626.

523 Derosiere G & Duque J (2020). Tuning the Corticospinal System: How Distributed Brain Circuits Shape
524 Human Actions. *The Neuroscientist* **26,** 359–379.

525 Devanne H, Lavoie BA & Capaday C (1997). Input-output properties and gain changes in the human
526 corticospinal pathway. *Exp Brain Res* **114,** 329–338.

527 Duque J, Greenhouse I, Labruna L & Ivry RB (2017). Physiological Markers of Motor Inhibition during
528 Human Behavior. *Trends Neurosci* **40,** 219–236.

529 Ferguson KA & Cardin JA (2020). Mechanisms underlying gain modulation in the cortex. *Nat Rev*
530 *Neurosci* **21,** 80–92.

531 Foltys H, Sparing R, Boroojerdi B, Krings T, Meister IG, Mottaghy FM & Töpper R (2001). Motor control in
532 simple bimanual movements: a transcranial magnetic stimulation and reaction time study. *Clinical*
533 *Neurophysiology* **112,** 265–274.

534 Frings C, Hommel B, Koch I, Rothermund K, Dignath D, Giesen C, Kiesel A, Kunde W, Mayr S, Moeller B,
535 Möller M, Pfister R & Philipp A (2020). Binding and Retrieval in Action Control (BRAC). *Trends Cogn*
536 *Sci* **24,** 375–387.

537 Georgopoulos AP & Stefanis CN (2007). Local shaping of function in the motor cortex: Motor contrast,
538 directional tuning. *Brain Res Rev* **55,** 383–389.

539 Greenhouse I (2022). Inhibition for gain modulation in the motor system. *Exp Brain Res* **240,** 1295–1302.

540 Greenhouse I, Sias A, Labruna L & Ivry RB (2015). Nonspecific Inhibition of the Motor System during
541 Response Preparation. *Journal of Neuroscience* **35,** 10675–10684.

542 Griffin DM & Strick PL (2020). The motor cortex uses active suppression to sculpt movement. *Sci Adv*;
543 DOI: 10.1126/sciadv.abb8395.

544 Halassa MM & Sherman SM (2019). Thalamocortical Circuit Motifs: A General Framework. *Neuron* **103,**
545 762–770.

546 Hannah R, Cavanagh SE, Tremblay S, Simeoni S & Rothwell JC (2018). Selective Suppression of Local
547 Interneuron Circuits in Human Motor Cortex Contributes to Movement Preparation. *The Journal of*
548 *Neuroscience* **38,** 1264–1276.

549 Hatsopoulos NG & Suminski AJ (2011). Sensing with the Motor Cortex. *Neuron* **72,** 477–487.

550 Heusser K, Heusser R, Jordan J, Urechie V, Diedrich A & Tank J (2021). Baroreflex Curve Fitting Using a
551 WYSIWYG Boltzmann Sigmoidal Equation. *Front Neurosci*; DOI: 10.3389/fnins.2021.697582.

552 Hillyard SA, Vogel EK & Luck SJ (1998). Sensory gain control (amplification) as a mechanism of selective
553 attention: electrophysiological and neuroimaging evidence. *Philos Trans R Soc Lond B Biol Sci* **353,**
554 1257–1270.

555 Hommel B (2009). Action control according to TEC (theory of event coding). *Psychological Research*
556 *Psychologische Forschung* **73,** 512–526.

557 Ibáñez J, Hannah R, Rocchi L & Rothwell JC (2020). Premovement Suppression of Corticospinal
558 Excitability may be a Necessary Part of Movement Preparation. *Cerebral Cortex* **30,** 2910–2923.

559 Jackson N & Greenhouse I (2019). VETA: An Open-Source Matlab-Based Toolbox for the Collection and
560 Analysis of Electromyography Combined With Transcranial Magnetic Stimulation. *Front Neurosci*;
561 DOI: 10.3389/fnins.2019.00975.

562 Katzner S, Busse L & Carandini M (2011). $GABA_A$ Inhibition Controls Response Gain in Visual Cortex.
563 *The Journal of Neuroscience* **31,** 5931–5941.

Kaufman MT, Churchland MM, Santhanam G, Yu BM, Afshar A, Ryu SI & Shenoy K V. (2010). Roles of Monkey Premotor Neuron Classes in Movement Preparation and Execution. *J Neurophysiol* **104,** 799–810.

Kaufman MT, Churchland MM & Shenoy K V. (2013). The roles of monkey M1 neuron classes in movement preparation and execution. *J Neurophysiol* **110,** 817–825.

Kukke SN, Paine RW, Chao C-C, de Campos AC & Hallett M (2014). Efficient and Reliable Characterization of the Corticospinal System Using Transcranial Magnetic Stimulation. *Journal of Clinical Neurophysiology* **31,** 246–252.

Di Lazzaro V, Oliviero A, Profice P, Insola A, Mazzone P, Tonali P & Rothwell JC (1999). Effects of voluntary contraction on descending volleys evoked by transcranial electrical stimulation over the motor cortex hand area in conscious humans. *Exp Brain Res* **124,** 525–528.

Lee S-H, Kwan AC, Zhang S, Phoumthipphavong V, Flannery JG, Masmanidis SC, Taniguchi H, Huang ZJ, Zhang F, Boyden ES, Deisseroth K & Dan Y (2012). Activation of specific interneurons improves V1 feature selectivity and visual perception. *Nature* **488,** 379–383.

Merchant H, Naselaris T & Georgopoulos AP (2008). Dynamic Sculpting of Directional Tuning in the Primate Motor Cortex during Three-Dimensional Reaching. *The Journal of Neuroscience* **28,** 9164–9172.

Mischler G, Keshishian M, Bickel S, Mehta AD & Mesgarani N (2023). Deep neural networks effectively model neural adaptation to changing background noise and suggest nonlinear noise filtering methods in auditory cortex. *Neuroimage* **266,** 119819.

Mitchell SJ & Silver RA (2003). Shunting Inhibition Modulates Neuronal Gain during Synaptic Excitation. *Neuron* **38,** 433–445.

586 Mukherjee A, Lam NH, Wimmer RD & Halassa MM (2021). Thalamic circuits for independent control of
587 prefrontal signal and noise. *Nature* **600,** 100–104.

588 Nambu A, Tokuno H & Takada M (2002). Functional significance of the cortico–subthalamo–pallidal
589 'hyperdirect' pathway. *Neurosci Res* **43,** 111–117.

590 Pi H-J, Hangya B, Kvitsiani D, Sanders JI, Huang ZJ & Kepecs A (2013). Cortical interneurons that
591 specialize in disinhibitory control. *Nature* **503,** 521–524.

592 Polack P-O, Friedman J & Golshani P (2013). Cellular mechanisms of brain state–dependent gain
593 modulation in visual cortex. *Nat Neurosci* **16,** 1331–1339.

594 Pouget A & Snyder LH (2000). Computational approaches to sensorimotor transformations. *Nat Neurosci*
595 **3,** 1192–1198.

596 Prut Y & Fetz EE (1999). Primate spinal interneurons show pre-movement instructed delay activity.
597 *Nature* **401,** 590–594.

598 Rabinowitz NC, Willmore BDB, Schnupp JWH & King AJ (2011). Contrast Gain Control in Auditory
599 Cortex. *Neuron* **70,** 1178–1191.

600 Salinas E & Sejnowski TJ (2001). Book Review: Gain Modulation in the Central Nervous System: Where
601 Behavior, Neurophysiology, and Computation Meet. *The Neuroscientist* **7,** 430–440.

602 Salinas E & Thier P (2000). Gain Modulation. *Neuron* **27,** 15–21.

603 Seki K & Fetz EE (2012). Gating of Sensory Input at Spinal and Cortical Levels during Preparation and
604 Execution of Voluntary Movement. *The Journal of Neuroscience* **32,** 890–902.

605 Shine JM, Aburn MJ, Breakspear M & Poldrack RA (2018). The modulation of neural gain facilitates a
606 transition between functional segregation and integration in the brain. *Elife*; DOI:
607 10.7554/eLife.31130.

608 Silbert BI, Patterson HI, Pevcic DD, Windnagel KA & Thickbroom GW (2013). A comparison of relative-
609 frequency and threshold-hunting methods to determine stimulus intensity in transcranial magnetic
610 stimulation. *Clinical Neurophysiology* **124,** 708–712.

611 Silver RA (2010). Neuronal arithmetic. *Nat Rev Neurosci* **11,** 474–489.

612 Soteropoulos DS (2018). Corticospinal gating during action preparation and movement in the primate
613 motor cortex. *J Neurophysiol* **119,** 1538–1555.

614 Stroud JP, Porter MA, Hennequin G & Vogels TP (2018). Motor primitives in space and time via targeted
615 gain modulation in cortical networks. *Nat Neurosci* **21,** 1774–1783.

616 Treue S & Trujillo JCM (1999). Feature-based attention influences motion processing gain in macaque
617 visual cortex. *Nature* **399,** 575–579.

618 Wang X, Liu Y, Li X, Zhang Z, Yang H, Zhang Y, Williams PR, Alwahab NSA, Kapur K, Yu B, Zhang Y,
619 Chen M, Ding H, Gerfen CR, Wang KH & He Z (2017). Deconstruction of Corticospinal Circuits for
620 Goal-Directed Motor Skills. *Cell* **171,** 440-455.e14.

621 Welniarz Q, Dusart I & Roze E (2017). The corticospinal tract: Evolution, development, and human
622 disorders. *Dev Neurobiol* **77,** 810–829.

623 Wood KC, Blackwell JM & Geffen MN (2017). Cortical inhibitory interneurons control sensory processing.
624 *Curr Opin Neurobiol* **46,** 200–207.

625 Xu J, Mawase F & Schieber MH (2024). Evolution, biomechanics, and neurobiology converge to explain
626 selective finger motor control. *Physiol Rev* **104,** 983–1020.

627 Zagha E, Ge X & McCormick DA (2015). Competing Neural Ensembles in Motor Cortex Gate Goal-
628 Directed Motor Output. *Neuron* **88,** 565–577.

629